34.0 PHASE AND TEXTURE EVOLUTION PRECEDING ABNORMAL GRAIN GROWTH IN NI-BASED AEROSPACE ALLOYS

Byron McArthur (Mines)
Faculty: Amy Clarke (Mines) and Kester Clarke (Mines)
Industrial Mentors: Eric Payton (AFRL), Kevin Severs (ATI)

This project initiated in Fall 2017 and is advised by Amy Clarke and Kester Clarke at Colorado School of Mines (Mines). The research performed during this project will serve as the basis for a Ph.D. thesis for Byron McArthur.

34.1 Project Overview and Industrial Relevance

Nickel-based superalloys are utilized extensively in the aerospace industry for their excellent high temperature strength, fatigue life, oxidation resistance and corrosion resistance. Turbine engine discs are flight critical components, and failure of these components risks loss of the entire aircraft. With the continuous push for more efficient commercial aviation, higher operating temperatures and pressures are desired. Complex Ni-based superalloys are being processed through novel methods to meet these stringent requirements.

The alloy utilized in the present study is RR1000, a γ-γ' disk alloy with approximately 45% volume fraction of γ' at room temperature. Processing steps for this alloy include alloyed powderization, hot isostatic pressing and extrusion at a 4.5:1 reduction ratio [34.1]. These steps produce a fully dense, recrystallized billet with γ grain size of 1-5 µm diameter and a distribution of primary γ' (γ_1', 1-3 µm) and secondary γ' (γ_2', 20-50 nm). Two material conditions provided are shown in **Figure 34.1**, note the significant difference in fraction of γ_1'. Subsequent isothermal deformation processing of slices of material is performed near the γ' solvus temperature; γ_2' is dissolved while γ_1' pins the γ grain boundaries and superplastic deformation keeps flow stresses low. Super-solvus heat treatment (SSHT), performed after isothermal forging, allows for γ growth to approximately 50 µm for increased creep resistance during service [34.1]. Abnormal grain growth (AGG) has been shown to occur during the SSHT step, and varies based upon processing parameters in the isothermal deformation (ε, $\dot{\varepsilon}$, T) and SSHT heating rate. The AGG results in γ grains up to 3 mm that compromise mechanical performance and are difficult to detect via non-destructive testing. The objective of this project is to better understand the microstructural mechanisms that cause AGG in these materials.

34.2 Previous Work

34.2.1 Literature Review

Prior research into AGG has been most successful in exploring the processing parameters required to produce AGG in an effort to prevent the phenomena from occurring in industrial settings. Huron et al. [34.2] performed double cone isothermal compression testing on a similar alloy (René 88DT) and found a range of strain rates and deformation temperatures that produce AGG; increasing deformation temperature required higher strain rates to produce AGG. Parr et al. [34.3] did similar testing on RR1000 and found AGG conditions to occur at near-γ'-solvus deformation temperatures, low strain rates, and low strains; similar to those explored in the present study. In-depth work performed by Payton [34.4] explored characterization techniques in an effort to understand the microstructural mechanism behind AGG; results indicated stored energy within the γ grains was a likely contribution to AGG, however combined contributions from γ' coherency changes and redistribution are important as well.

Work further exploring the AGG mechanisms has been performed by Charpagne et al. [34.5], and proposes that stored energy is the driving force for AGG, with static recrystallization of γ grains initiating the process. The recrystallization of the γ grains has been proposed by Charpagne to occur coherently off of γ_1', followed by growth to consume neighboring γ grains containing stored energy; this mechanism has been termed 'heteroepitaxial recrystallization' (HERX). The coherency allows for a reduced energy barrier for recrystallization of the γ, theoretically occurring at lower temperatures. Interestingly, the γ grain boundaries appear to pass through large γ_1' with relatively low Zener pinning influence. Charpagne's work demonstrated continued growth of γ grains within critical regions until impingement upon each other limited grain growth. This suggests the final grain size is determined by the number of nucleation sites that then grow to consume regions of unrecrystallized grains. The nucleation limited growth may be explained by inhomogenous distributions of stored energy that is a precursor to static recrystallization. Tu et al.'s work [34.6] supports this through strain mapping characterization techniques demonstrating significant grain-to-grain

variations in plastic strain accumulation as well as changes in deformation mechanisms near the critical strain rates required for AGG. Based upon prior research, it appears that stored energy, accumulated inhomogeneously during isothermal forging, creates the precursor requirements for AGG.

34.2.2 Thermomechanical Processing to Produce Abnormal Grain Growth

Prior experiments in this study focused on establishing the thermomechanical processing parameters for consistently producing AGG in the experimental RR1000 materials. The main portion of this research so far has focused on the material with the starting condition shown in **Figure 34.1a**, containing a lower fraction of γ_1', smaller γ_2' and larger γ grains, as this material has shown instances of AGG during testing. Thermomechanical processing of the material with the starting condition shown in **Figure 34.1b** has not yet demonstrated instances of AGG. This is likely due to increased amounts of γ_1' influencing the deformation and recrystallization.

Isothermal compression of RR1000 specimens was performed in a Gleeble® thermomechanical simulator. This allowed for control of deformation temperature, strain, and strain rate as well as providing load-displacement data. Post-deformation SSHT of the material utilized a TA Instruments quenching dilatometer to maintain precise temperature and heating rate control, as well as measure qualitative γ' dissolution and γ grain growth behavior through changes in length. The deformation temperature, strain rate, and strain utilized in the Gleeble® to produce AGG were 1110°C, 0.0008 ε/s and 0.16 ε, respectively. This is just below the 1135-1145°C γ' solvus temperature. Utilizing the dilatometer, a low heating rate (0.12°C/s) up to the SSHT temperature (1170°C) promoted AGG occurrence.

The results from the present study support a mechanism akin to the HERX mechanism previously described; though, it is still uncertain of the origin of the nuclei that leads to AGG. The strain and strain rate during isothermal forging impart a stored energy that may provide the driving force for AGG nuclei to grow, yet insufficient for traditional, homogeneous recrystallization. The slow heating rate during SSHT may allow for recovery in the γ and slow dissolution of the γ_1' to form stable AGG nuclei. The γ_1' phase fraction, size, and distribution appear to be of importance, as observed from the sensitivity of the two starting conditions of material to creating AGG. While the γ_2' are dissolved at isothermal forging and heat treating temperatures, the γ_1' exists and serves as AGG nuclei location sites.

34.3 Recent Progress

34.3.1 Strain Rate Sensitivity Testing

Isothermal forging of the material at different strain rates and temperatures was performed in the Gleeble® to correlate processing parameters, deformation mechanisms, and post-deformation stored energy. A temperature range of 1040°C to 1140°C was utilized to capture the region of industrial processing, abnormal grain growth, and γ' solvus temperature (1135°C). Jump testing using strain rates varying from 10^{-2} to 10^{-4} s^{-1} during compression allowed for comparison of the material's response to deformation. Strain rate sensitivity was calculated from the ratio of change in flow stress for a change in strain rate. Interestingly, strain rate sensitivity dropped with increasing temperature approaching the γ' solvus temperature, shown in **Figure 34.2**. This is thought to be due to γ grain size increasing as the pinning second phase dissolves, shifting from superplastic grain-boundary sliding to dislocation interaction and multiplication. This corroborates with an increased flow stress observed with increasing temperatures near the γ' solvus performed in an earlier report [34.8].

34.3.2 Observing Interfaces via Diffusion Bonding

Interrupted heat treatments of RR1000 to observe the γ-γ' interface during γ' dissolution proved difficult due to the γ_1' size (~1-5µm) relative to the polishing techniques required between interrupted heat treatments on the polished surface. Additionally, relying upon statistics to find and track an AGG nuclei (hypothesized to be at the γ-γ_1' interface) throughout the steps of recrystallization and growth encouraged alternative techniques. A Ni_3Al button of stoichiometric composition was arc-melted (and remelted 5 times) then homogenized in a quartz capsuleat 1000°C for 24 hours. A section of the Ni_3Al button and Ni200 (99.8% Ni, 0.2% C) specimen were prepared to a 1µm diamond polished surface then diffusion bonded in a dilatometer at 1000°C for 4 hours in an argon purged, 10^{-6} Torr vacuum. This was performed in an effort to represent the local microstructure at the γ-γ_1' interface during γ_1' dissolution in RR1000 at a mesoscopic level. **Figure 34.3** shows the diffusion couple at the interface. As previously observed by

Watanabe [34.9] and Kawazoe [34.10], diffusion reduced the aluminum content of the Ni_3Al side and the γ' near the prior interface lost ordering to become γ, yet maintained its parent γ' orientation. This new γ could act as a suitable nuclei for recrystallization in a deformed γ-γ' alloy. The stability of the new γ during continued dissolution of the γ' and γ grain growth is of importance to the AGG theory presented by this work.

34.4 Plans for Next Reporting Period

Upcoming efforts will continue focusing on diffusion couple experiments. To create pre-SSHT conditions in a diffusion coupled experiment, adding deformation to the γ portion (prior to diffusion coupling) would provide the driving force for growth of the AGG nuclei. A sufficient amount of strain energy is required, yet still below the critical amount for traditional, homogeneous recrystallization. To accomplish this, specimens of Ni200 and IN-625 (a solid solution strengthened Ni-based superalloy) were strained to 5, 10, and 15% elongation then sectioned into diffusion couple specimens for the dilatometer. Tensile testing was chosen to produce a homogeneous distribution of strain within the material, and IN-625 was chosen as an alternative single phase γ alloy due to higher temperature recrystallization than Ni200. It is hypothesized that the Ni_3Al (γ') will transform to γ near the interface and the new γ will grow to consume the γ grains with stored energy in the Ni200/IN-625.

If this hypothesis is confirmed, subsequent testing will focus on providing methods for preventing AGG in an industrial setting. It is further hypothesized that several techniques may be viable; (1) performing a post-isothermal forging 'bump' at higher strain rates to impart additional stored energy into the material homogeneously (via superplasticity), (2) decreasing the isothermal forging temperature, and (3) heating above the γ' solvus temperature as a last step to isothermal forging.

34.5 References

[34.1] M. C. Hardy, B. Zirbel, G. Shen, R. Shankar. Developing damage tolerance and creep resistance in a high strength nickel alloy for disc applications, Superalloys 2004 83 (2004).

[34.2] E. Raymond, E. Huron, S. Srivasta. Control of grain size via forging strain rate rimits for R'88DT, Superalloys 49 (2000).

[34.3] I. M. D. Parr, T. J. Jackson, M. C. Hardy, D. J. Child, C. Argyrakis, K. Severs, V. Saraf, J. M. Stumpf. Inhomogeneous grain coarsening behavior in supersolvus heat treated nickel-based superalloys RR1000, Superalloys 447 (2016).

[34.4] E. J. Payton, Characterization and modeling of grain coarsening in powder metallurgical nickel-based superalloys, The Ohio State University (2009).

[34.5] M. A. Charpagne, J. M. Franchet, N. Bozzolo. Overgrown grains appearing during sub-solvus heat treatment in a polycrystalline γ-γ' Nickel-based superalloy, Mater. Des. 144, 353 (2018).

[34.6] W. Tu, T. M. Pollock. Grain scale straining processes during high temperature compression of a PM disk alloy, Superalloys 395 (2008).

[34.7] E.R. Homer, V. Tikare, E.A. Holm, Hybrid Potts-phase field model for coupled microstructural – compositional evolution, 69 414–423 (2013).

[34.8] B. McArthur, A. Clarke, K. Clarke, Phase and texture evolution preceding abnormal grain growth in ni-based aerospace alloys, CANFSA Fall 2018 Report (2018).

[34.9] M. Watanabe, Z. Horita, D.J. Smith, M.R. McCartney, T. Sano, M. Nemoto, Electron microscopy study of Ni/Ni3Al diffusion-couple interface-I. Microstructural observation and microchemical analysis, Acta Metall. Mater. 42 3381–3387 (1994).

[34.10] H. Kawazoe, Morphological and crystallographic features of y-y ' Ni-AI and Ni-AI-Ti two-phase bicrystals, J. Mater. Sci. 17, 1303–1310 (1982).

34.6 Figures and Tables

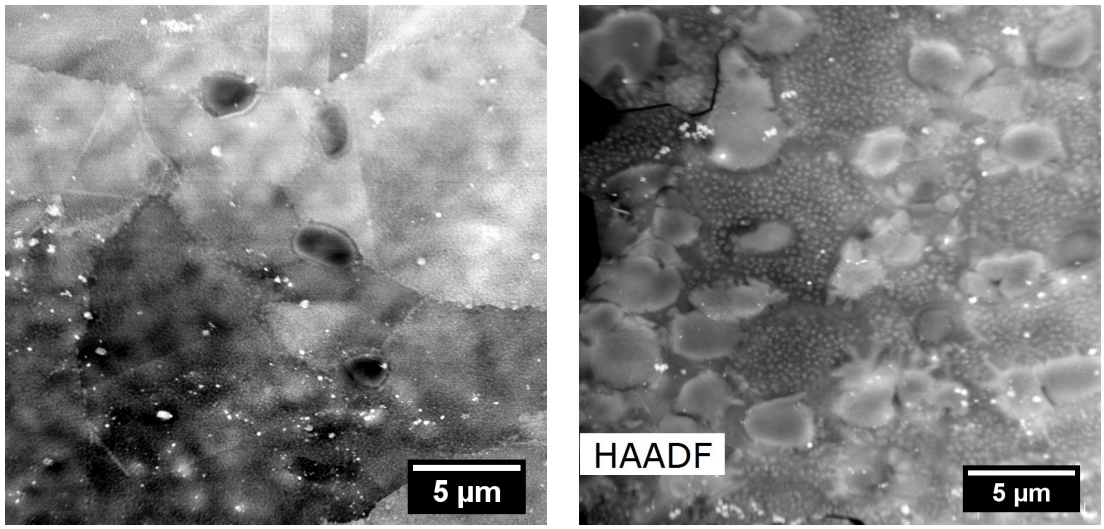

a) b)

Figure 34.1: TEM micrographs of starting material conditions for 'Slice' 1 (a) and 2 (b) in Bright Field (BF) and High Angle Anular Dark Field (HAADF) imaging modes, respectively. Slice 1 has γ_1' shown in darker regions, with γ_2'dispersed throughout the γ grains. Slice 2 shows higher volume fraction of γ_1' and larger γ_2'. Note the lighter regions are likely carbides and halfnia clusters remaining in the material as well as redeposited during electropolishing (Image courtesy of help from Yaofeng Gao, Mines).

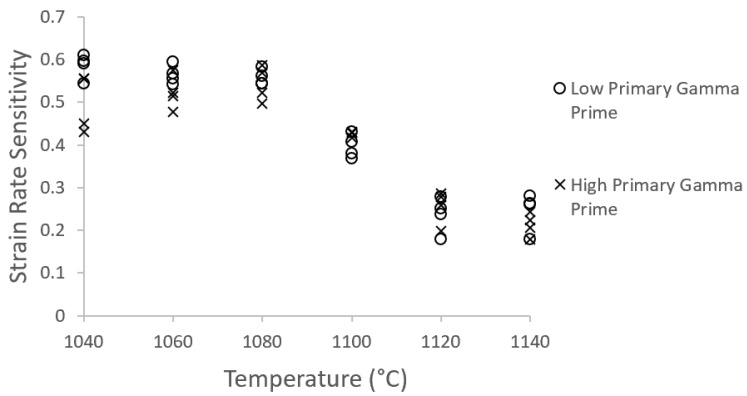

Figure 34.2: Strain rate sensitivity versus temperature for both starting microstructure conditions. Note the decrease in strate rate sensitivity as temperature approaches the 1135°C γ' solvus temperature. Data points taken from jump load testing between 10^{-4} to 10^{-2} s^{-1} strain rates.

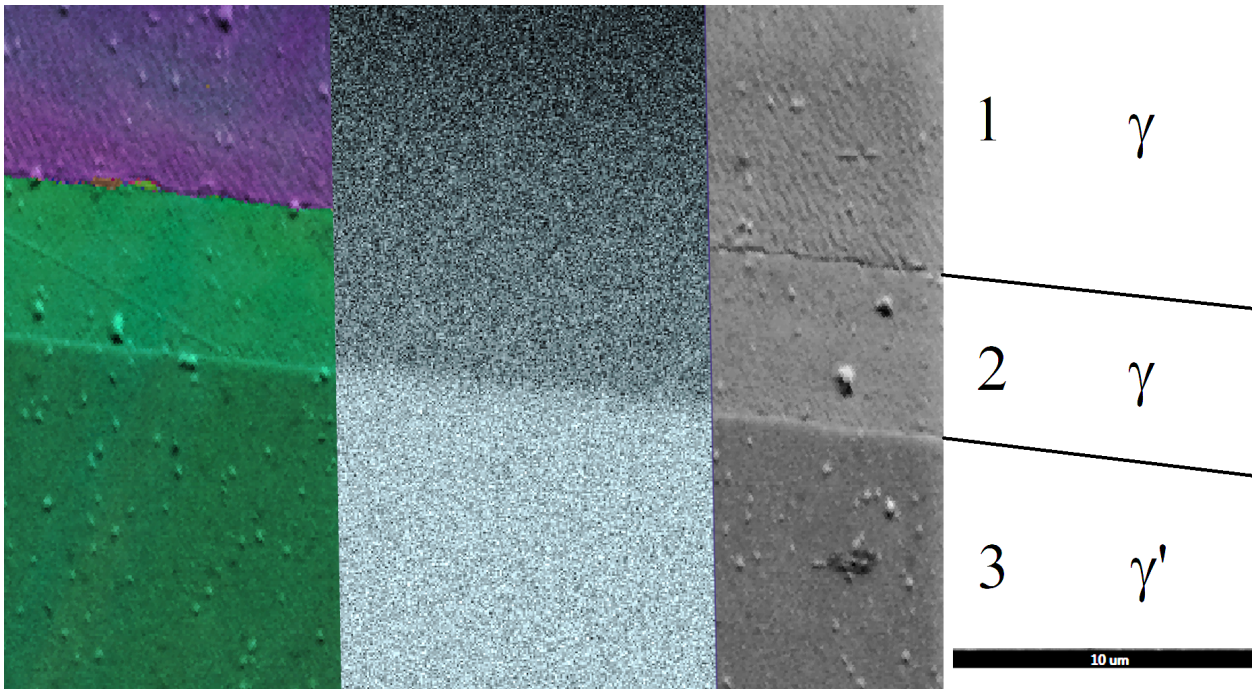

Figure 34.3: Micrograph of diffusion couple interface.The leftmost part of the image is an EBSD overlay illustrating regions 2 and 3 of the same orientation. The middle part of the image shows an EDS elemental map overlay for aluminum in teal illustrating a diffuse decreasing gradient from region 2 through 1 and a sharp gradient between region 2 and 3. The rightmost part of the image shows a secondary electron image of the sectioned and mechanically polished surface. Note the initial interface between the nickel and Ni3Al specimens is between regions 1 and 2.